LIGHT-HADRON ELECTROPRODUCTION AT NEXT-TO-LEADING ORDER AND IMPLICATIONS

BERND A. KNIEHL

II. Institut für Theoretische Physik, Universität Hamburg,
Luruper Chaussee 149, 22761 Hamburg, Germany
E-mail: kniehl@desy.de

We review recent results on the inclusive electroproduction of light hadrons at next-to-leading order in the parton model of quantum chromodynamics implemented with fragmentation functions and present updated predictions for HERA experiments based on the new AKK set. We also discuss phenomenological implications of these results.

1. Introduction

In the framework of the parton model of quantum chromodynamics (QCD), the inclusive production of single hadrons is described by means of fragmentation functions (FFs) $D_a^h(x,\mu)$. At lowest order (LO), the value of $D_a^h(x,\mu)$ corresponds to the probability for the parton a produced at short distance $1/\mu$ to form a jet that includes the hadron h carrying the fraction x of the longitudinal momentum of a. Analogously, incoming hadrons and resolved photons are represented by (non-perturbative) parton density functions (PDFs) $F_a^h(x,\mu)$. Unfortunately, it is not yet possible to calculate the FFs from first principles, in particular for hadrons with masses smaller than or comparable to the asymptotic scale parameter Λ. However, given their x dependence at some energy scale μ, the evolution with μ may be computed perturbatively in QCD using the timelike Dokshitzer-Gribov-Lipatov-Altarelli-Parisi (DGLAP) equations. Moreover, the factorization theorem guarantees that the $D_a^h(x,\mu)$ functions are independent of the process in which they have been determined and represent a universal property of h. This entitles us to transfer information on how a hadronizes to h in a well-defined quantitative way from e^+e^- annihilation, where the measurements are usually most precise, to other kinds of experiments, such as photo-, lepto-, and hadroproduction. Recently, FFs for light charged hadrons with complete quark flavour separation were determined[1] through

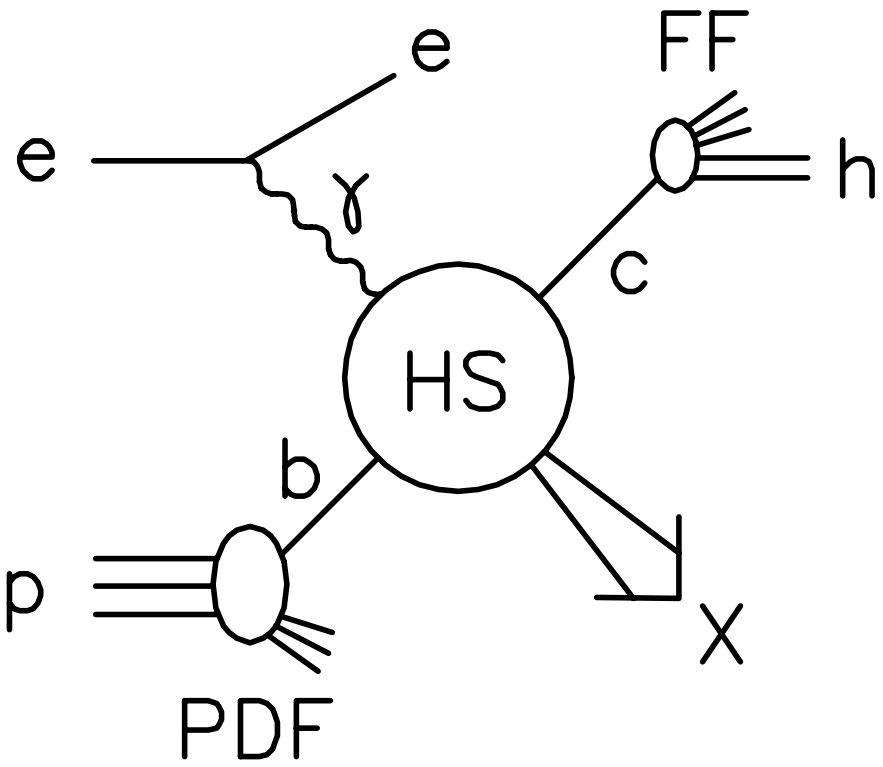

Figure 1. Parton-model representation of $ep \to eh + X$.

a global fit to e^+e^- data from LEP, PEP, and SLC including for the first time the light-quark tagging probabilities measured by the OPAL Collaboration at LEP,[2] thereby improving previous analyses.[3,4]

The QCD-improved parton model should be particularly well applicable to the inclusive production of light hadrons carrying large transverse momenta (p_T) in deep-inelastic lepton-hadron scattering (DIS) with large photon virtuality (Q^2) due to the presence of two hard mass scales, with $Q^2, p_T^2 \gg \Lambda^2$. In Fig. 1, this process is represented in the parton-model picture. The hard-scattering (HS) cross sections, which include colored quarks and/or gluons in the initial and final states, are computed in perturbative QCD. They were evaluated at LO more than 25 years ago.[5] Recently, the next-to-leading-order (NLO) analysis was performed independently by three groups.[6,7,8] A comparison between Refs. 7, 8 using identical input yielded agreement within the numerical accuracy.

The cross section of $e^+p \to e^+\pi^0 + X$ in DIS was measured in various distributions with high precision by the H1 Collaboration at HERA in the forward region, close to the proton remnant.[9,10] This measurement reaches down to rather low values of Bjorken's variable $x_B = Q^2/(2P\cdot q)$, where P and q are the proton and virtual-photon four-momenta, respectively, and $Q^2 = -q^2$, so that the validity of the DGLAP evolution might be challenged by Balitsky-Fadin-Kuraev-Lipatov (BFKL) dynamics.

In Ref. 7, the H1 data[9,10] were compared with NLO predictions evaluated with the KKP FFs.[3] In Sec. 2, we summarize the analytical calculation performed in Ref. 7. In Sec. 3, we present an update of this comparison based on the new AKK FFs.[1] Our conclusions are summarized in Sec. 4.

2. Analytical calculation

The partonic subprocesses contributing at LO are

$$\begin{aligned}
&\gamma^* + q \to q + g,\\
&\gamma^* + q \to g + q,\\
&\gamma^* + g \to q + \overline{q},
\end{aligned} \tag{1}$$

where q represents any of the n_f active quarks or antiquarks and it is understood that the first of the final-state partons is the one that fragments into the hadron h.

At NLO, processes (1) receive virtual corrections, and real corrections arise through the partonic subprocesses

$$\begin{aligned}
&\gamma^* + q \to q + g + g,\\
&\gamma^* + q \to g + q + g,\\
&\gamma^* + g \to q + \overline{q} + g,\\
&\gamma^* + g \to g + q + \overline{q},\\
&\gamma^* + q \to q + q + \overline{q},\\
&\gamma^* + q \to \overline{q} + q + q,\\
&\gamma^* + q \to q + q' + \overline{q}',\\
&\gamma^* + q \to q' + \overline{q}' + q,
\end{aligned} \tag{2}$$

where $q' \neq q, \overline{q}$. The virtual corrections contain infrared (IR) singularities, both of the soft and/or collinear types, and ultraviolet (UV) ones, which are all regularized using dimensional regularization with $D = 4 - 2\epsilon$ space-time dimensions yielding poles in ϵ in the physical limit $D \to 4$. The

latter arise from one-loop diagrams and are removed by renormalizing the strong-coupling constant and the wave functions of the external partons in the respective tree-level diagrams, while the former partly cancel in combination with the real corrections. The residual IR singularities are absorbed into redefinitions of the PDFs and FFs. We extract the IR singularities in the real corrections by performing the phase space integrations using the dipole subtraction formalism.[11]

3. Comparison with H1 data

We work in the modified minimal-subtraction ($\overline{\rm MS}$) renormalization and factorization scheme with $n_f = 5$ massless quark flavors and identify the renormalization and factorization scales by choosing $\mu^2 = \xi[Q^2 + (p_T^*)^2]/2$, where the asterisk labels quantities in the $\gamma^* p$ center-of-mass (c.m.) frame and ξ is varied between 1/2 and 2 about the default value 1 to estimate the theoretical uncertainty. At NLO (LO), we employ set CTEQ6M (CTEQ6L1) of proton PDFs,[12] the NLO (LO) set of AKK FFs,[1] and the two-loop (one-loop) formula for the strong-coupling constant $\alpha_s^{(n_f)}(\mu)$ with $\Lambda^{(5)} = 226$ MeV (165 MeV).[12]

The H1 data[9,10] were taken in DIS of positrons with energy $E_e = 27.6$ GeV on protons with energy $E_p = 820$ GeV in the laboratory frame, yielding a c.m. energy of $\sqrt{S} = 2\sqrt{E_e E_p} = 301$ GeV. The DIS phase space was restricted to $0.1 < y < 0.6$ and $2 < Q^2 < 70$ GeV^2, where $y = Q^2/(x_B S)$. The π^0 mesons were detected within the acceptance cuts $p_T^* > 2.5$ GeV (except where otherwise stated), $5^\circ < \theta < 25^\circ$, and $x_E > 0.01$, where θ is their angle with respect to the proton flight direction and $E = x_E E_p$ is their energy in the laboratory frame. The comparisons with our updated LO and NLO predictions are displayed in Figs. 2(a)–(d). The QCD correction (K) factors, i.e. the NLO to LO cross section ratios, are presented in the downmost frame of each figure.

Comparison of Figs. 2(a)–(d) with Figs. 3, 5(a), 6(c), and 7 in Ref. 7, where the KKP FFs[3] were used, reveals that the update of our FFs, from set KKP to set AKK,[1] has hardly any visible impact on the theoretical predictions considered here. This may be understood by observing that the OPAL light-quark tagging probabilities for charged pions,[2] included in the AKK analysis, agree well with the assumption made in the KKP one that $D_u^{\pi^\pm}(x,\mu_0) = D_d^{\pi^\pm}(x,\mu_0)$ at the starting scale μ_0 of the DGLAP evolution. In Figs. 3(a) and (b),[8] the H1 data[10] on $d\sigma/dp_T^*$ for $2 < Q^2 < 4.5$ GeV^2, $4.5 < Q^2 < 15$ GeV^2, or $15 < Q^2 < 70$ GeV^2 and on $d\sigma/dx_B$ for $p_T^* >$

3.5 GeV and $2 < Q^2 < 8$ GeV^2, $8 < Q^2 < 20$ GeV^2, or $20 < Q^2 < 70$ GeV^2, respectively, are compared with the LO and NLO predictions evaluated with the KKP FFs[3] or those by Kretzer (K).[4] While the LO predictions based on the KKP and K sets agree very well, the NLO predictions based on the K set appreciably undershoot those based on the KKP set. If it were not for the theoretical uncertainty, one might conclude that the H1 data prefer the KKP set at NLO.

From the downmost frames in Figs. 2(a)–(d), we observe that the K factors are rather sizeable, although the μ values are reasonably large. In Fig. 4,[8] the impact of the H1 forward-selection cuts on the K factor is studied for the case of $d\sigma/dx_B$ for $2 < Q^2 < 8$ GeV^2 and $p_T^* > 3.5$ GeV. Towards the lower end of the considered x_B range, the K factor reaches one order of magnitude if these cuts are imposed [see also Fig. 2(c)]. However, if the latter are removed, the K factor collapses to acceptable values of around 3. From this finding, we conclude that these cuts almost quench the LO cross section. In other words, in the extreme forward regime, the latter is effectively generated by the $2 \to 3$ partonic subprocesses of Eq. (2).

It is interesting to investigate the relative importance of the *tagged* partons, i.e. the one (a) that originates from the proton and the one (b) that fragments into the hadron. In Fig. 5,[8] the NLO contributions from the four most important ab channels to $d\sigma/dx_B$ for $2 < Q^2 < 8$ GeV^2 and $p_T^* > 3.5$ GeV with the H1 forward-selection cuts are shown together with the total LO contribution. We observe that the gg channel makes up approximately two thirds of the cross section in the low-x_B regime.

4. Conclusions

We calculated the cross section of $ep \to e\pi^0 + X$ in DIS for finite values of p_T^* at LO and NLO in the parton model of QCD[7] using the new AKK FFs[1] and compared it with a precise measurement by the H1 Collaboration at HERA.[9,10]

We found that our LO predictions always significantly fell short of the H1 data and often exhibited deviating shapes. However, the situation dramatically improved as we proceeded to NLO, where our default predictions, endowed with theoretical uncertainties estimated by moderate unphysical-scale variations, led to a satisfactory description of the H1 data in the preponderant part of the accessed phase space. In other words, we encountered K factors much in excess of unity, except towards the regime of asymptotic freedom characterized by large values of p_T^* and/or Q^2. This was

unavoidably accompanied by considerable theoretical uncertainties. Both features suggest that a reliable interpretation of the H1 data within the QCD-improved parton model ultimately necessitates a full next-to-next-to-leading-order analysis, which is presently out of reach, however. For the time being, we conclude that the successful comparison of the H1 data with our NLO predictions provides a useful test of the universality and the scaling violations of the FFs, which are guaranteed by the factorization theorem and are ruled by the DGLAP evolution equations, respectively.

Significant deviations between the H1 data and our NLO predictions only occurred in certain corners of phase space, namely in the photoproduction limit $Q^2 \to 0$, where resolved virtual photons are expected to contribute, and in the limit $\eta \to \infty$ of the pseudorapidity $\eta = -\ln[\tan(\theta/2)]$, where fracture functions are supposed to enter the stage. Both refinements were not included in our analysis. Interestingly, distinctive deviations could not be observed towards the lowest x_B values probed, which indicates that the realm of BFKL dynamics has not actually been accessed yet.

Acknowledgments

The author thanks G. Kramer and M. Maniatis for their collaboration. This work was supported in part by BMBF Grant No. 05 HT1GUA/4.

References

1. S. Albino, B. A. Kniehl and G. Kramer, *Nucl. Phys.* **B725**, 181 (2005); *Nucl. Phys.* **B734**, 50 (2006).
2. OPAL Collaboration, G. Abbiendi et al., *Eur. Phys. J.* **C16**, 407 (2000).
3. B. A. Kniehl, G. Kramer and B. Pötter, *Nucl. Phys.* **B582**, 514 (2000); *Phys. Rev. Lett.* **85**, 5288 (2000); *Nucl. Phys.* **B597**, 337 (2001).
4. S. Kretzer, *Phys. Rev.* **D62**, 054001 (2000).
5. A. Mendez, *Nucl. Phys.* **B145**, 199 (1978).
6. P. Aurenche, R. Basu, M. Fontannaz and R. M. Godbole, *Eur. Phys. J.* **C34**, 277 (2004).
7. B. A. Kniehl, G. Kramer and M. Maniatis, *Nucl. Phys.* **B711**, 345 (2005); **B720**, 231(E) (2005).
8. A. Daleo, D. de Florian and R. Sassot, *Phys. Rev.* **D71**, 034013 (2005).
9. H1 Collaboration, C. Adloff et al., *Phys. Lett.* **B462**, 440 (1999).
10. H1 Collaboration, A. Aktas et al., *Eur. Phys. J.* **C36**, 441 (2004).
11. S. Catani and M. H. Seymour, *Nucl. Phys.* **B485**, 291 (1997); **B510**, 503(E) (1997).
12. J. Pumplin, D. R. Stump, J. Huston, H.-L. Lai, P. Nadolsky and W.-K. Tung, *JHEP* **0207**, 012 (2002).

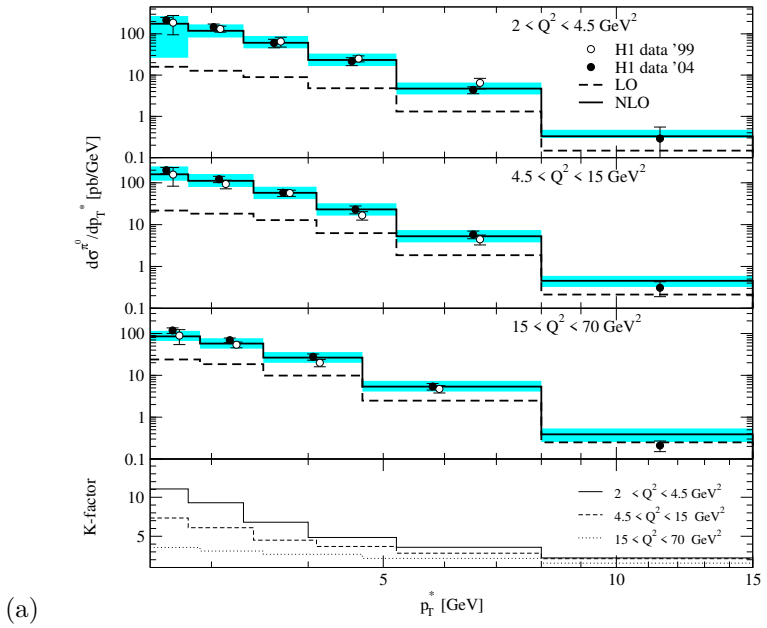

(a)

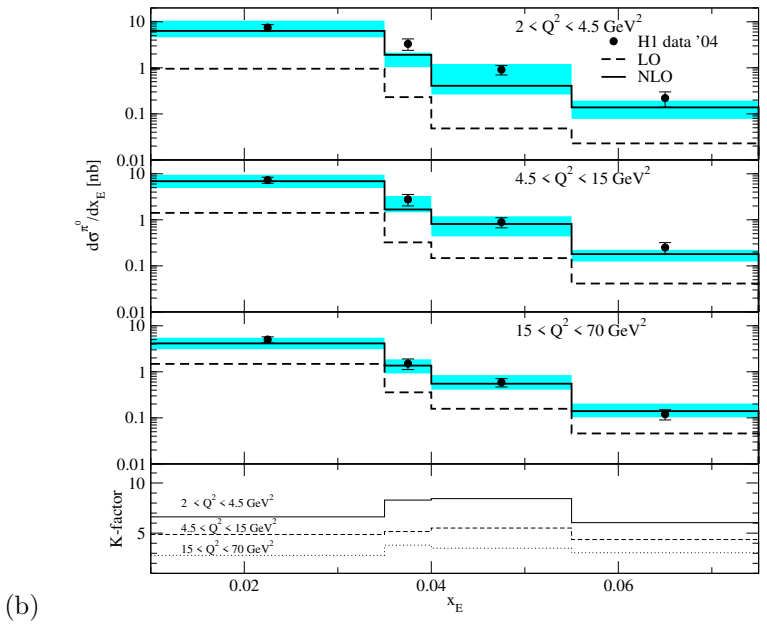

(b)

Figure 2. H1 data on (a) $d\sigma/dp_T^*$ and (b) $d\sigma/dx_E$ for $2 < Q^2 < 4.5$ GeV^2, $4.5 < Q^2 < 15$ GeV^2, or $15 < Q^2 < 70$ GeV^2, on (c) $d\sigma/dx_B$ for $p_T^* > 3.5$ GeV and $2 < Q^2 < 8$ GeV^2, $8 < Q^2 < 20$ GeV^2, or $20 < Q^2 < 70$ GeV^2, and on (d) $d\sigma/dQ^2$ from Refs. 9 (open circles) and 10 (solid circles) are compared with our default LO (dashed histograms) and NLO (solid histograms) predictions including theoretical uncertainties (shaded bands). The K factors are also shown.

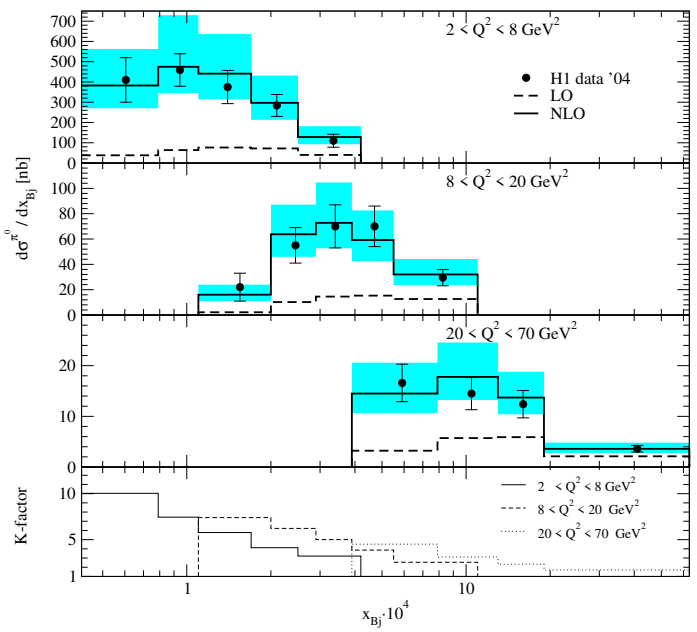

(c)

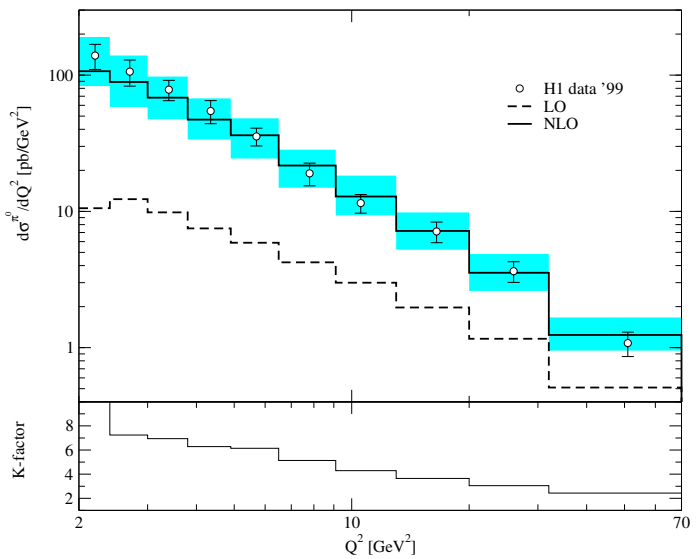

(d)

Figure 2. Continued.

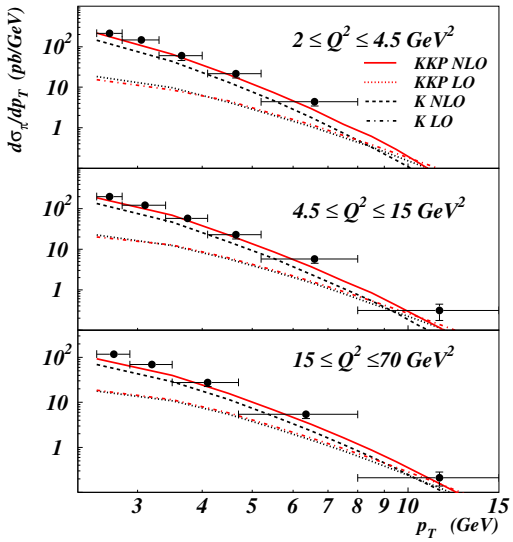

(a)

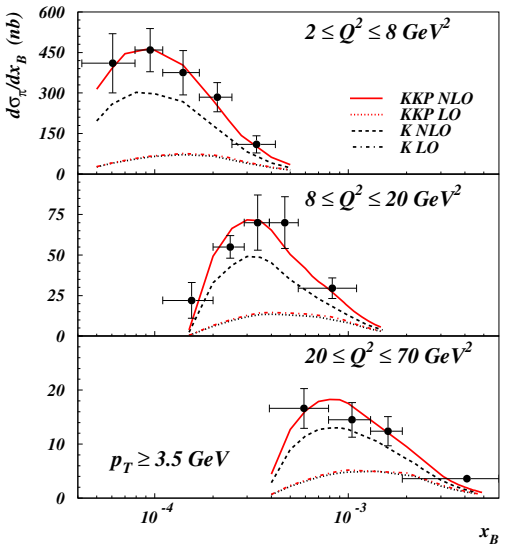

(b)

Figure 3. H1 data[10] on (a) $d\sigma/dp_T^*$ for $2 < Q^2 < 4.5$ GeV^2, $4.5 < Q^2 < 15$ GeV^2, or $15 < Q^2 < 70$ GeV^2 and on (b) $d\sigma/dx_B$ for $p_T^* > 3.5$ GeV and $2 < Q^2 < 8$ GeV^2, $8 < Q^2 < 20$ GeV^2, or $20 < Q^2 < 70$ GeV^2 are compared with the LO and NLO predictions evaluated with the KKP[3] or K[4] FFs (taken from Ref. 8).

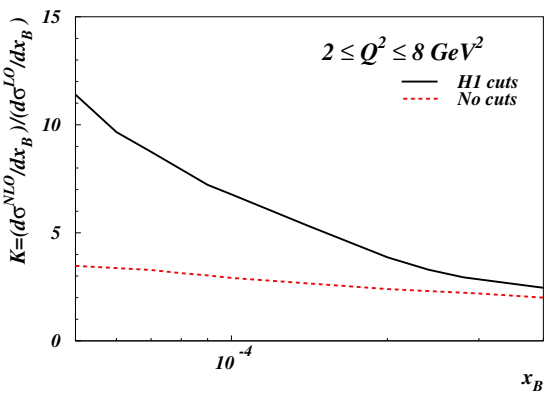

Figure 4. K factors of $d\sigma/dx_B$ for $2 < Q^2 < 8$ GeV^2 and $p_T^* > 3.5$ GeV with and without the H1 forward-selection cuts[10] (taken from Ref. 8).

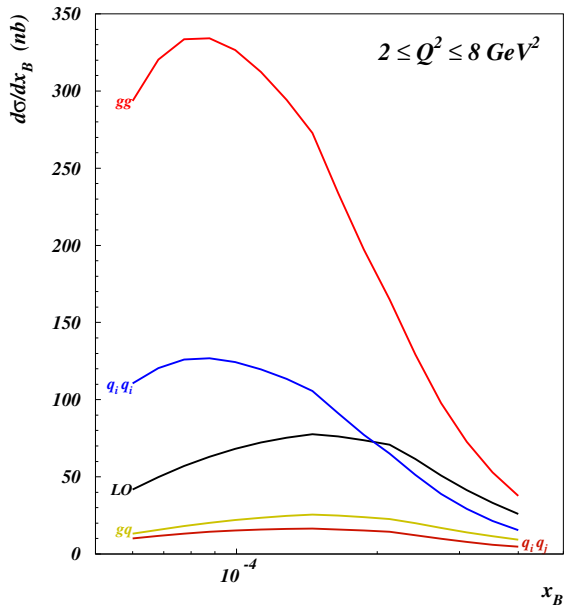

Figure 5. Total LO contribution and NLO contributions from the four most important ab channels, where a and b are the partons connected with the PDFs and FFs, respectively, to $d\sigma/dx_B$ for $2 < Q^2 < 8$ GeV^2 and $p_T^* > 3.5$ GeV with the H1 forward-selection cuts[10] (taken from Ref. 8).